Cement & Concrete Composites 48 (2014) 108–117

Contents lists available at ScienceDirect

Cement & Concrete Composites

journal homepage: www.elsevier.com/locate/cemconcomp

Influence of starting material on the early age hydration kinetics, microstructure and composition of binding gel in alkali activated binder systems

Elisabeth Deir [a], Berhan S. Gebregziabiher [a], Sulapha Peethamparan [b,*]

[a] Department of Civil and Environmental Engineering, Clarkson University, 8 Clarkson Avenue, Box 5712, Potsdam, NY 13699, USA
[b] Department of Civil and Environmental Engineering, Clarkson University, 8 Clarkson Avenue, Box 5710, Potsdam, NY 13699, USA

ARTICLE INFO

Article history:
Received 13 July 2013
Received in revised form 19 November 2013
Accepted 28 November 2013
Available online 6 December 2013

Keywords:
Fly ash
Slag
Alkali activation
Calorimetry
SEM
EDX

ABSTRACT

The influence of starting material on the hydration kinetics and composition of binding gel in alkali activated binder systems was evaluated. The starting materials used were ground granulated blast furnace slag, class C fly ash and class F fly ash. All starting materials were activated using alkaline solution with a SiO_2/Na_2O ratio of 1.5. The hydration kinetics were monitored using in situ isothermal conduction calorimetry and the chemical compositions of the binder gels were determined by energy dispersive X-ray spectroscopy. In the fly ash systems, the calorimetric curves had only one peak, which occurred in the first 30 min of reaction, and lacked an induction period. Two peaks were distinguishable in slag systems, though the induction period was much shorter than that of a typical OPC system. The gel composition ratios, including Ca/Si, Na/Si, Na/Al and Al/Si, were different in each of the systems and are discussed in detail.

1. Introduction

Industrial by products such as ground granulated blast furnace slag (also called GGBFS or slag) and fly ash have been used for many years to supplement ordinary Portland cement (OPC) in concrete binders [1–5]. In addition to improving properties and performance of concrete, their inclusion lowers the cost and energy required to produce one of the most commonly used construction materials [2,6,7]. Furthermore, the CO_2 emission attributed to the production of concrete binder, approximately one ton CO_2 per ton cement [8–10], decreases with increasing supplementary cementitious material (SCM) incorporation.

The growing concern regarding the effects of CO_2 emissions from cement plants, in conjunction with continued desire to improve the durability of concrete, has motivated many studies on developing alternative binders for concrete in the past several decades [11]. Formulating these new binders involves replacing 50–100 wt.% of the cement with SCM's instead of the typical replacement level within 10–50 wt.%. In the case of 100% cement replacement, alkalis are needed for activation of the starting materials [12]. When sodium silicate is used in the alkaline activator, the environmental benefits expected of these binding systems have been found to be offset by the negative environmental impact of sodium silicate in categories other than global warming potential [13].

A highly alkaline solution, called an activator, provides a high pH environment (pH > 12) that facilitates dissolution of the reactive (vitreous) phases of the starting material into the surrounding solution. Recent studies have found that, in properly designed mixtures and conditions, the dissolved ionic species reorient, react, and polycondensate to form a three dimensional network of hydraulically and dimensionally stable products that has potential to function as a binder in concrete [6,14].

Though many studies have reported on alkali activation of class F fly ash and slag, and a general agreement regarding the types of reaction products can be seen in these studies, only a few studies have been conducted on class C fly ash based binders [15–17]. The main product resulting from alkali activation of class F fly ash is reported to be an alkali aluminosilicate, or N–A–S–(H), gel regardless of the type of activator used [15,18]. This gel is characterized by a lack of medium- and long-range order and the possession of short range order (consisting of polymer chains of

Abbreviations: C-FA, class C fly ash; F-FA, class F fly ash; Slag, ground granulated blast furnace slag; SM, silica modulus that is SiO_2/Na_2O molar ratio; s:sm, solution-to-starting material ratio.

* Corresponding author. Tel.: +1 315 268 4435 (w); fax: +1 315 268 7985 (f).
E-mail addresses: deirer@clarkson.edu (E. Deir), gebregbs@clarkson.edu (B.S. Gebregziabiher), speetham@clarkson.edu (S. Peethamparan).

0958-9465/$ - see front matter © 2013 Elsevier Ltd. All rights reserved.
http://dx.doi.org/10.1016/j.cemconcomp.2013.11.010

tectosilicates incorporating aluminum tetrahedra and charge balancing alkali) whose structure resembles that of zeolitic precursors [18]. In contrast, the main reaction products in alkali-activated slag systems consist of C–(A)–S–H gel with different proportions of Ca to Si compared with those of OPC systems, and possibly hydrotalcite-like products ($Mg_6Al_2(CO_3)(OH)_{16}{\cdot}4(H_2O)$) [4,16,19], though this is a point of some debate. In the case of class C fly ash, whose composition lies between that of class F fly ash and slag, N–A–S–(H) and C–(A)–S–H gels have been found to coexist when activated using mildly elevated temperatures and sodium silicate solution with a silica modulus (SM) of $SiO_2/Na_2O = 1.5$ [17]. Alkali-activated binders stemming from class F and class C fly ashes have also been found to contain minor amounts of secondary products in the form of various zeolite phases [18].

Though the same type of gel (N–A–S–(H) or C–(A)–S–H) product is formed under a range of conditions (for example, temperature, solution/binder ratio, solution concentration) for a given starting material, the mechanical strength of alkali-activated binders depends, to varying degrees, on several factors [4,6,14]. Among the most influential factors are the type and concentration of the activator used [14,15]. These have been found to affect the reaction kinetics, microstructural development, and composition of the products of reaction [14,20,21]. The activator types most commonly used to activate fly ash and slag include sodium hydroxide solution and sodium silicate solution. Sodium carbonates are also commonly used to activate slag, but result in poor strength development in the case of fly ash based systems [15]. Increasing the activator concentration and curing temperature has been found to increase the initial reaction rate and generally lead to higher early age strength [22]. Alkali activation of fly ash and slag using properly-formulated sodium silicate solution has been found to yield superior results compared to those of activation using sodium hydroxide solution [17,18].

Though numerous studies investigating the effect of activator type, activator concentration and curing conditions on different sources of an individual type of starting material have been published [15–17,19,22,23], studies comparing the effect of these variables on completely different types of starting materials are not comprehensive. Some examples include van Jaarsveld et al.'s investigation of the effect of activator type and concentration on the composition of reaction products formed in alkali-activated fly ash/kaolin based systems [24]. Bernal et al. studied the effect of slag–metakaolin starting material blends on the evolution of binder structure in sodium silicate-activated systems [25]. Ravikumar [22] explored the effect of activator concentration on the compressive strength, porosity, and microstructure of sodium hydroxide-activated slag and class F fly ash. Oh et al. studied the effect of sodium hydroxide and sodium silicate activators on the strength and crystalline phase development in fly ash and slag-based geopolymeric binders cured at 80 °C [26].

The present study adds to the understanding of the effect of starting material type on the early-age reaction kinetics, compressive strength development, microstructure and binding gel composition of alkali activated concrete binders. Alkaline solution containing sodium silicate and soluble sodium hydroxide species is used to activate GGBFS, class C fly ash, and class F fly ash. The type and concentration of the activators, as well as the mixture proportioning and curing condition parameters used were selected with the intent of creating hardened binders of appreciable compressive strength from each of the starting materials. The findings of this study offer information on the efficiency of this type of alkaline solution to activate various starting materials for creating cement free concrete with a wide range of compressive strengths. The results also provide a useful comparison of hardened state gel product composition of alkali activated binders based on starting material type. In-situ isothermal calorimetry is used for investigating the reaction kinetics. To date, most of the published calorimetric studies of geopolymerization employ either metakaolin or a mixture of metakaolin, ordinary Portland cement, fly ash, and other starting materials [27]; though an occasional isothermal calorimetric study of alkali hydroxide-activated fly ash has been published [28]. Metakaolin is typically the preferred material for geopolymerization calorimetry studies because of its compositional and morphological homogeneity and thus its conduciveness to replicable results. This study investigates the usefulness of in-situ isothermal conduction calorimetry for identifying the relative setting time, strength development and microstructural development of alkaline-activated fly ash- and slag-based binders.

2. Materials and methods

In the present study, three different starting materials were combined individually with two different activating solutions to form six unique pastes. After being mixed, these pastes were prepared for compressive strength testing and microstructural characterization. The net rate and extent of heat evolved from the reactions of each paste was also studied.

2.1. Materials

The starting materials used in this study included a ground granulated blast furnace slag (also known as GGBFS or slag)[1], a class C fly ash (C-FA)[1], and a class F fly ash (F-FA)[1]. The chemical oxide composition of each powder is provided in Table 1. The oxide composition (wt.%) was analyzed using a Bruker AXS S4 Explorer XRF. The particle size distribution of each powder, determined using a laser particle size analyzer (Malvern Mastersizer 2000), is shown in Fig. 1. The average particle size of the slag, C-FA, and F-FA was 7.5 μm, 6.5 μm, and 10.0 μm, respectively.

Two alkaline solutions with the same silica modulus (SiO_2/Na_2O molar ratio; SM) of 1.5 but different sodium oxide (and silicon dioxide) concentrations were used separately to activate each of the three starting materials. These activating solutions were prepared using solid sodium hydroxide microbeads (99.99% purity), a reagent grade sodium silicate solution (with density 1.39 g/mL, and ~10.6 and ~26.5 wt.% of Na_2O and SiO_2; respectively), and water (tap water for compressive strength and BSEM/EDS specimens and deionized water for isothermal conduction calorimetry). They were formulated such that, when mixed at an activating

Table 1
Chemical composition of starting materials.

Component	Wt.%		
	Slag	Class C fly ash	Class F fly ash
CaO	39.1	21.07	5.29
SiO_2	37.8	40.68	48.07
Al_2O_3	7.91	21.20	23.03
MgO	10.3	3.99	0.98
Na_2O	0.30	1.53	0.69
Fe_2O_3	0.43	5.44	14.42
SO_3	2.60	1.95	0.96
K_2O	0.47	0.68	1.73
P_2O_5	<0.01	1.08	0.35
TiO_2	0.39	0.68	0.52
MnO	0.50	0.02	0.02
SrO	0.05	0.37	0.08
BaO	<0.01	0.60	0.13
ZrO_2	0.04	0.04	0.04
CeO_2	<0.01	<0.01	0.06
CoO	<0.01	<0.01	0.03
LOI[a]	0.0	0.31	3.36

[a] Accounts for loss due to C, CO_2, H_2O, OH, organic compounds and/or other.

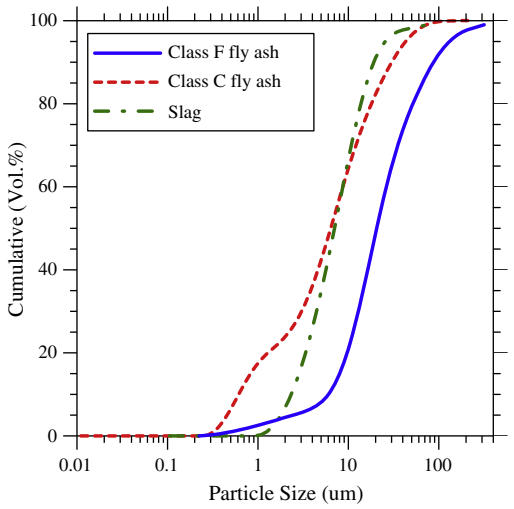

Fig. 1. Particle size distribution of the class F fly ash, class C fly ash, and slag used for this study.

solution-to-starting material (s/sm) ratio of 0.45, they contributed either 5 wt.% Na_2O (7.5 wt.% soluble SiO_2) or 7 wt.% Na_2O (10.5 wt.% soluble SiO_2) by mass of starting material to the paste. The composition and pH of each activating solution used in this study is given in Table 2 below. The pH was measured using a bench top pH meter (Denver Instrument UB-5) with a pH resolution of 0.01 and a pH accuracy of 0.005. Henceforth, the cured pastes formed by mixtures of one of the starting materials with one of these two activating solutions will be referred to as "5% Na_2O slag" and "7% Na_2O slag," for example, respectively. It should be kept in mind that each activator contains 150% as much soluble silica as it does sodium oxide, though only the sodium oxide content is used to refer to a given activator throughout this work.

2.2. Methods

2.2.1. Sample preparation

In order to prepare each of the F-FA pastes studied in this work for compressive strength testing and microstructure characterization, the activating solution was added to the starting material at a solution-to-starting material ratio of 0.45 within 30 s and the two mixture components were hand mixed together at slow speed (about 100 ± 5 rpm) for 30 s. The mixture was then allowed to rest for 30 s before being mixed again for 1 min, this time at a medium speed (approx. 150 ± 5 rpm). The paste was then poured into 50 mm Plexiglas cube molds for compressive strength testing (3 specimens per mixture) and cylindrical 31.75 mm diameter molds for characterization studies. These molded specimens were then compacted on a vibrating table until medium and large air voids ceased breaking through the top surface, about 1 to 2 min. The compressive strength test specimens were subsequently finished with a flat trowel. All specimens were sealed using a layer of plastic wrap followed by a layer of aluminum foil and placed in a precision laboratory oven set to 50 °C ± 1 °C. The slag pastes were prepared in the same manner as the F-FA pastes were, except that an automatic mixer was used instead of hand mixing. The slag specimens were allowed to cure for 1 day and the F-FA specimens for 2 days. These durations were chosen to maximize compressive strength development for these specimens at 50 °C ± 1 °C within a curing time frame restricted to a maximum of 2 days.

Due to the extremely brief setting time of the C-FA based pastes (under three minutes), they required a different mixing procedure from that used for pastes made with the other two starting materials. Instead of mixing for a total of 90 s with rest in between mixing segments, the C-FA pastes were mixed for 60 s and then transferred immediately to molds. Following these steps, the specimens were prepared according to the procedure outlined for F-FA and slag specimens and were cured at 50 °C ± 1 °C for 2 days, like the F-FA specimens.

2.2.2. Compressive strength testing

After being removed from the oven, all compressive strength specimens were cooled on a lab bench for at least one hour before being demolded, weighed, measured, and the strength was determined as per ASTM C39.

2.2.3. Reaction kinetics

In-situ isothermal conduction calorimetry was employed for the purpose of qualitatively comparing between the kinetics of reaction of each of the six mixtures studied by measuring the heat evolved from each during its reaction. 1.013 g of activating solution was measured into a syringe and 2.252 g of starting material was measured into an in situ ampoule. The two components were equilibrated in the calorimeter's isothermal chamber at 50 °C. Once thermal equilibrium was reached, the activating solution was injected into the ampoule already containing the measured quantity of starting material and mixed for one minute. The heat flow and cumulative heat evolved by the paste was then recorded and normalized by the mass of the starting material (that is, slag, C-FA, or F-FA).

2.2.4. BSEM sample preparation and microstructure characterization

The hardened cylindrical specimens were cut to size (approx. 2 cc) using a diamond saw and submerged in a large amount of 2-Propanol for 3 days to quench their reaction. The cut samples were then dried in an oven at 50 °C for 3 days. Following this, the specimens were impregnated with epoxy and polished using 45 μm and 15 μm lapping pads and polishing cloths impregnated with diamond pastes of particle sizes ranging from 9 um to 0.25 um. Polished specimens were placed in vacuum desiccators until shortly prior to characterization using BSEM/EDX instruments. Shortly before characterization, the polished specimens were sputter coated with 60% Au/40% Pd. Specimens were then examined in backscatter mode under a field emission scanning electron microscope (FE-SEM). The elemental composition of the gel product was determined using an EDX analysis on the specimen's polished surface. Gel "points" were sampled at several locations distributed across the specimen's polished surface; one location at each corner and one in the center of the surface. Three to six gel points were sampled at each of these locations on the specimen surface at a magnification of 2500×. The center of each gel "point" sampled was located at least 1 μm away from all identified binder particle remnants (e.g. fly ash or slag particles), to avoid as much interference from unreacted particles in the EDX "point" composition as possible. However, the interference of the

Table 2
Composition and pH of alkaline activating solutions (SiO_2/Na_2O molar ratio = 1.5).

Activating solution name	SiO_2/Na_2O molar ratio	Na_2O (wt.%)	SiO_2 (wt.%)	H_2O (wt.%)	pH
5% Na_2O	1.5	11.11	16.67	72.22	12.96
7% Na_2O	1.5	15.56	23.33	61.11	13.16

particles underneath the gel points on the composition could not be avoided.

3. Results and discussion

3.1. Compressive strength

The compressive strength of the six cured paste mixtures is reported here to assist with interpretation and analysis of the results of the characterization efforts made in this study. Fig. 2 shows the strength results for slag-, C-FA- and F-FA-based binders prepared with the 5% Na_2O and 7% Na_2O alkaline activating solutions. The values shown for slag are those of specimens cured for 24 h, while those shown for fly ash are those of specimens cured for 48 h. From additional unpublished compressive strength tests conducted by the authors, it appears that slag systems at high Na_2O do not require elevated temperature to develop adequate strength and reach strengths of over 100 MPa by 28 days of curing. However, similar curing conditions are used here for comparison with fly ash-based alkali-activated systems. As is evident from Fig. 2, average compressive strengths of 119.8 MPa and 165.1 MPa were obtained for slag at 24 h of curing. However, it was noticed that a longer period of heat curing resulted in formation of numerous cracks in slag systems, and in significant reduction in strength. No such strength reduction was observed for C-FA or F-FA systems. On the contrary, both F-FA systems and the 5% Na_2O C-FA system increased in compressive strength and the 7% Na_2O C-FA system showed no significant difference in compressive strength with the increase in curing time from 24 h to 48 h.

Comparing mixtures activated with 5 wt.% and 7 wt.% Na_2O (contributing 7.5% and 10.5% SiO_2, respectively) solutions, it may be observed that the compressive strength of slag based and F-FA based mixtures both increase significantly with increasing activator concentration for the activator parameters used in this study. On the other hand, no significant difference in compressive strength is observed for C-FA based specimens prepared from the two activators. It may also be noted that the 5% Na_2O activator is not sufficient for development of compressive strength in excess of 30 MPa in the alkali activated F-FA system under the employed curing regimen. The same activator (5% Na_2O) yields excellent strength when combined with either of the other two starting materials. These observations suggest that higher dosage of activator is essential for activation and strength development of class F fly ash based binder cured at 50 °C. This result supports the results of previously published research conducted by Fernández-Jiménez and Palomo [15]. This is not to say that high pH is not essential for activation and strength development of C-FA and slag. Instead, the behaviors observed may indicate that the pH of the activating solution is increased by immediate dissolution of alkalis to a greater extent in the case of slag and C-FA than in the case of F-FA. This possibility is examined further in Section 3.4 (Gel Composition).

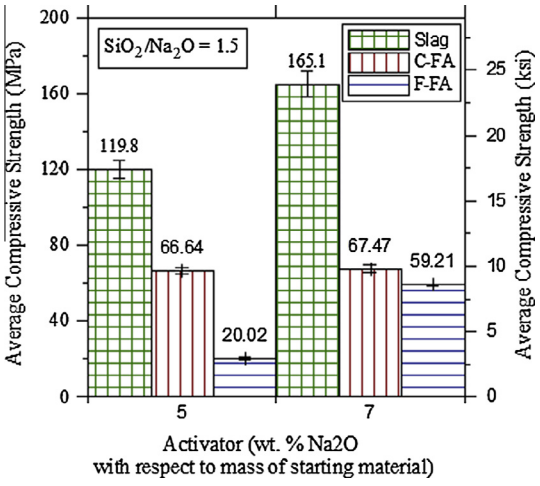

Fig. 2. Compressive strength vs. activating solution Na_2O concentration of alkali activated paste specimens prepared using slag, class C fly ash, and class F fly ash. All mixtures prepared were at a solution-to-starting material ratio of 0.45 and cured at 50 °C (122°F) for 1 (slag) or 2 (FA) days.

Also of interest is the observation that the compressive strength of these alkali activated materials increases with increasing calcium content in the starting materials; increasing progressively from class F fly ash based to class C fly ash based to slag based alkali activated binders. This strength correlation with calcium content has also been noted by other researchers [29]. One potential explanation for this trend is that calcium is readily dissociated into solution from the starting material particles along with silica and alumina. When this calcium becomes available in solution, various calcium silicate-based binding products have the potential to form. The available Ca would thus be less of a limiting factor in gel formation than available Al and Si for aluminosilicate product formation in the case of Ca-deficient systems. The influence of calcium on the different binding systems will be discussed subsequently in conjunction with analysis of the microstructural morphology and gel composition.

3.2. Reaction kinetics

In Fig. 3(a–d), the heat flow (normalized by mass of starting material) of the six pastes studied during reaction at 50 °C is shown over a period of four days. The portion of the plots that contains the most notable features is the first four hours of reaction, where peaks are observed. The graphs are broken between four hours and 80 h of reaction, because the profile of each of the curves only gradually decreases during this period. The last 16 h of reaction are plotted following the break.

It may be observed from the figures that each of the six curves shows an initial peak within the first 30 min of reaction. For a given activating solution, the C-FA paste exhibits the highest peak, followed by the slag paste, followed by the F-FA paste. The initial peak height increases by about 50% with the increase in activator concentration for the C-FA and slag pastes. In comparison, the initial peak height increases more drastically, by about 400%, for the F-FA pastes. This seems to indicate that, though dissolution of each material is sensitive to pH, dissolution of the vitreous phases in class F fly ash may require a higher-pH externally-provided environment than the other two starting materials. This trend of increased dissolution of the vitreous Si–O–Si and Si–O–Al bonds in fly ash with increasing pH supports the findings of previous researchers [15]. The initial peak height for C-FA paste compared with slag paste does not correlate with the strength development in C-FA paste compared to slag based mixtures. It is important to note, thus, that the reaction mechanisms are different for slag and fly ash activation.

As may be observed from Fig. 3, the F-FA and C-FA pastes' normalized heat flow curves only exhibit one initial peak, subsequently decreasing gradually, approaching but not reaching zero mW/g. In contrast, normalized heat flow curves for the slag pastes exhibit two peaks. This difference in heat flow profile indicates a difference in reaction mechanism between alkali-activated fly ash and slag based systems.

The calorimetric curves obtained for slag samples activated with 5% and 7% Na_2O 1.5SM solutions show the main stages of reactions that normally occur in the ordinary Portland cement (OPC) hydration process. These divisions are commonly known

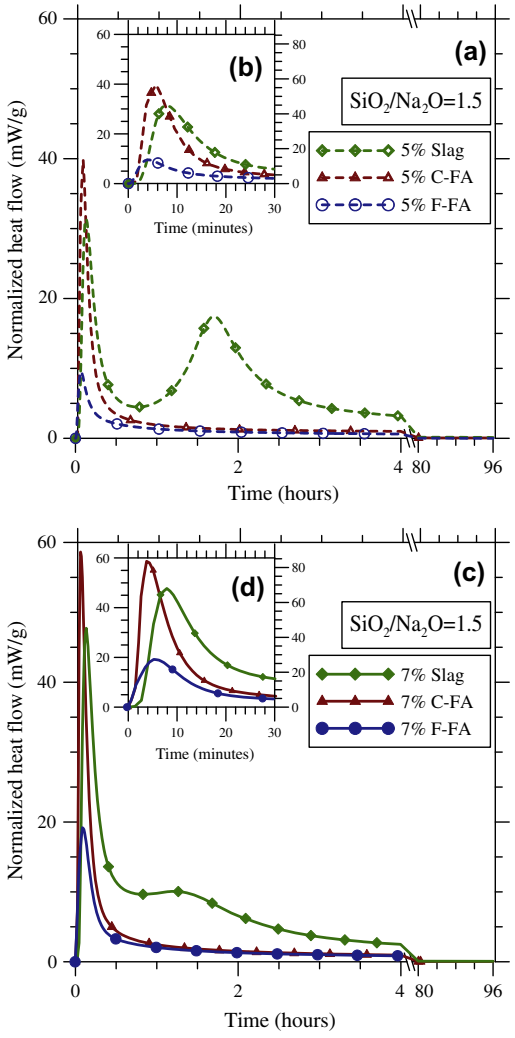

Fig. 3. (In-situ) Normalized heat flow of reaction for alkali-activated pastes prepared using different starting materials and activated by (a), (b) 5 wt.% Na_2O and (c), (d) 7 wt.% Na_2O alkaline solution (1.5SM, 0.45 s:sm[1], 50 °C), using isothermal conduction calorimetry.

to be the initial wetting, induction, rapid acceleration, deceleration and steady state periods. The main difference between 5% and 7% Na_2O-containing specimens appears to be that the presence of higher Na_2O in the system accelerates the reaction, providing a very short induction period and a higher peak during the wetting process. For 7% Na_2O, it can be readily observed from the hydration curve that the main reaction and the initial wetting almost overlap. The higher pH and higher percentage of Na_2O increases the spontaneity of the reaction, leading to one combined major peak occurring right after the addition of the solution into the slag powder. This condition allows for the formation of hydration product during the very early hours of the hydration process. Solution analysis of these systems (unpublished) show that Al continues to dissociate until an adequate amount of ions are available, followed by the formation of products consisting of Ca, Mg, Si, Na, and Al. Considering that slag is composed of 39.1 wt.% CaO, the pore solution is immediately rich in Ca, Si, and Na. With further dissociation of Al in the beginning of the hydration process, the systems continue forming products until a saturation point is reached or a steady state of hydration kinetics is obtained. Other studies have reported that higher alkalinity will result in higher Si and Al concentrations in the pore solution [30,31]. It is also reported that Ca solubility in a solution decreases at a higher pH, whereas Mg shows insignificant variation with change in pH of the solution that contains it.

In contrast to those of the slag-based systems, the heat flow curves of the fly ash-based systems apparently do not exhibit an induction period at all. Instead, the exothermic dissolution and polycondensation reactions proceed concurrently [18]. The presence of soluble silica in the activating solution facilitates the formation of aluminosilicate oligomers as soon as reactive aluminate from the fly ash particles becomes available in solution [32]. When these oligomers reach a high concentration, they react to form alkali aluminosilicate polymers, consisting of linked silica and alumina tetrahedra and alkali species. The alkali cations (that is, usually Na^+ and/or K^+) present in the activating solution are necessary for the formation of these polymers, as they serve to balance the negative charge on alumina tetrahedra (AlO_4^-) [33]. The initial rate of alumina dissolution is high in high-pH solution, and thus the concentration of monomer and oligomer species in solution builds rapidly, feeding prolific polycondensation that results in a short range-ordered 3-dimensional network structure [18]. The rapid rate of dissolution and polycondensation does not allow sufficient time for the oligomer species to organize enough to form medium- or long-range ordered molecular structure [34]. Over time, however, reorienting, reorganizing and further polymerization is thought to take place [6,18], accounting for the steady but low heat flow following the initial peak.

The cumulative normalized heat of reaction is shown in Fig. 4 for each of the six mixtures over the course of four days. Notice that the trends in the cumulative heat evolved correlate fairly well with the compressive strength trends for these mixtures (that is, after 1 and 2 days of curing at 50 °C). The slag based mixtures gave off about twice as much heat as their C-FA counterpart mixtures. The 5% Na_2O F-FA curve is significantly lower than that of the 7% Na_2O F-FA curve, while the 7% Na_2O curve is not far below those of the C-FA mixtures. There is very little difference in the 5% and 7% Na_2O C-FA mixture curves. However, the parallel between compressive strength and cumulative heat evolved apparently breaks down for the 5% and 7% Na_2O alkali-activated slag mixtures.

The curves plotting cumulative normalized heat evolved for 5% and 7% Na_2O, 1.5SM alkali-activated slag systems, shown in Fig. 4, indicate some differences occurring beginning at about 8 h of hydration. The main reason for this variation is the fast initial rate

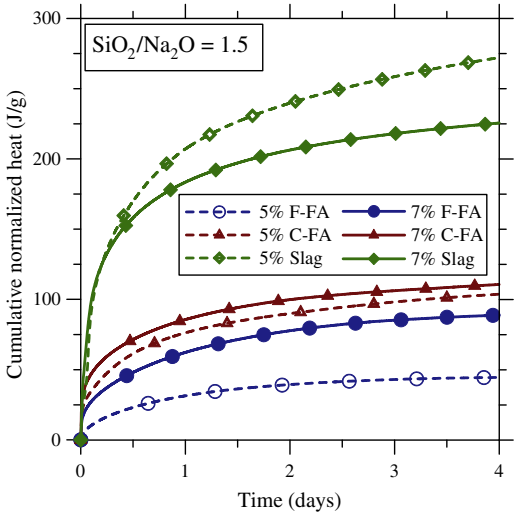

Fig. 4. (In situ) Cumulative normalized heat of reaction for alkali-activated pastes prepared using different starting materials (sm)[1] and activated by 5 wt.% and 7 wt.% Na_2O alkaline solution (1.5SM, 0.45 solution-to-starting material, 50 °C), using isothermal conduction calorimetry.

of reaction that resulted in immediate formation of products, which may inhibit the further dissolution of the unreacted slag grains into the pore solution. Another reason could be the insufficient amount of surrounding liquid for dissolution due to a reduced amount of pure water present in 7% Na_2O alkaline solution. Consequently, the total heat evolved for the 7% Na_2O alkali-activated slag comes to be lower than that for the 5% Na_2O alkali-silicate-activated slag system. Curing these samples at 25 °C (unpublished) resulted in a similar trend between 5% and 7% Na_2O alkali-activated slag systems. The similar sets of hydration curves for the different curing temperatures may imply that, for the 7% Na_2O alkali-activated slag system, the combined mechanism of high alkalinity and lower amount of free water reduces the degree of hydration at later times because of the faster reduction of mobility of ions. As a result, the 5% Na_2O alkali-activated slag system shows an increase relative to the 7% Na_2O alkali-activated slag system in the cumulative heat evolved after 24 h.

Comparing the cumulative heat curves of the alkali-activated F-FA and C-FA based geopolymerization reactions with their corresponding compressive strength values, we see that the compressive strength trends match those of the calorimetric curves. 7% Na_2O C-FA evolves slightly more heat than 5% Na_2O C-FA, 7% Na_2O F-FA evolves slightly less heat than 5% Na_2O C-FA, and there is a more significant gap between 7% Na_2O F-FA and 5% Na_2O F-FA, corresponding with the measured compressive strength trends reported earlier. From these results, it seems that isothermal calorimetry data can be correlated with mechanical strength behavior (which is related to microstructural development) of the alkali-activated fly ash-based geopolymer paste and may therefore be a useful supplementary tool for investigating the relative behavior of other fly ashes when activated with similar alkaline solutions. Since fly ash composition varies widely based on the source of the coal it is derived from and furnace and handling conditions that vary between and within power plants, isothermal calorimetric studies may be useful for comparing the behavior of various fly ashes under identical activation conditions. Further studies are necessary to validate this observed correlation for other activating solution silica moduli and for other activator-to-starting material ratios.

3.3. Microstructure

Figs. 5(a–f) and 6(a–f) show backscatter mode scanning electron micrograph (BSEM) images of the slag (a and b), C-FA (c and d), and F-FA (e and f) based binders characterized in this study, activated with 5 wt.% and 7 wt.% Na_2O, 1.5SM alkaline solution, respectively. The pair of images that corresponds with each starting material show representative areas of the polished composite at two magnifications (500× and 1000×) to give a couple of different views of the material that has formed. Here, one may observe the well-established microstructure of hardened alkali activated binder with unreacted slag and fly ash particles embedded in an apparently continuous gel matrix connecting the unreacted portions of the starting material grains together. The radial phase separation in fly ash particles noted by other researchers in the past is clearly evident, particularly in F-FA particles [35]. It is also noticeable that there is a greater variety of particles with different chemical composition in the class C fly ash compared to that in the class F fly ash, and that

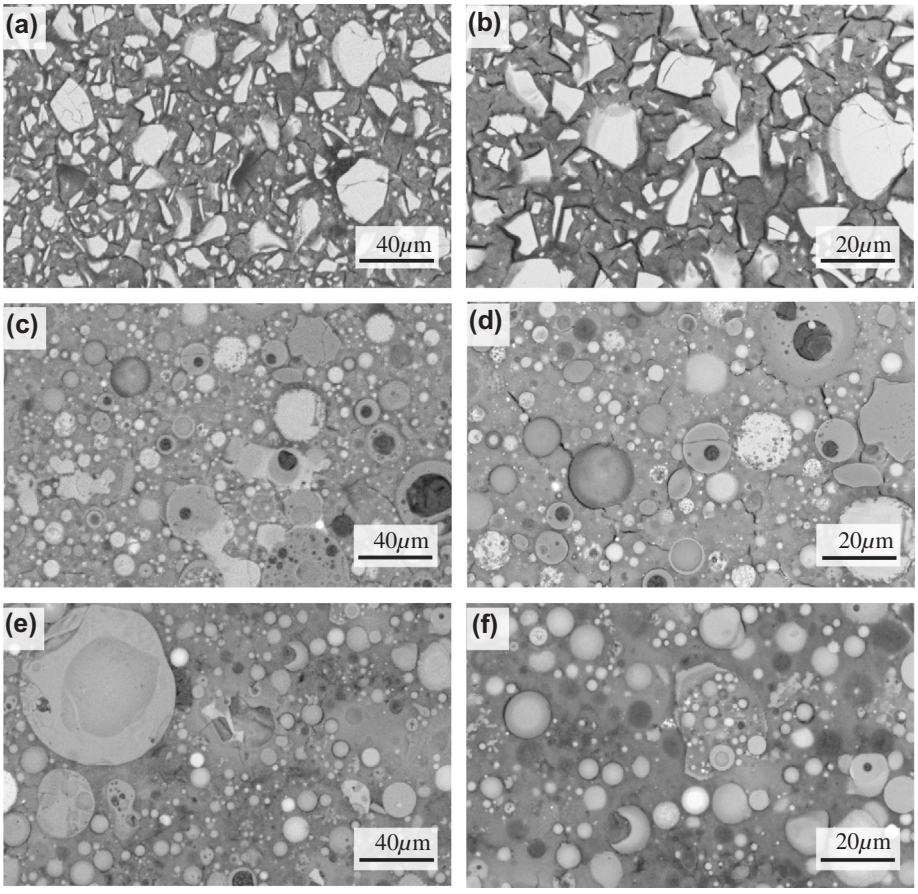

Fig. 5. Backscatter SEM mode images of alkali-activated binder formed from slag (a and b), class C fly ash (c and d), and class F (e and f) fly ash mixed with alkaline solution that contributes 5 wt.% Na_2O (1.5 SM) with respect to starting material at a solution-to-starting material ratio of 0.45, and curing for (a and b) 1 or (c–f) 2 days at 50 °C.

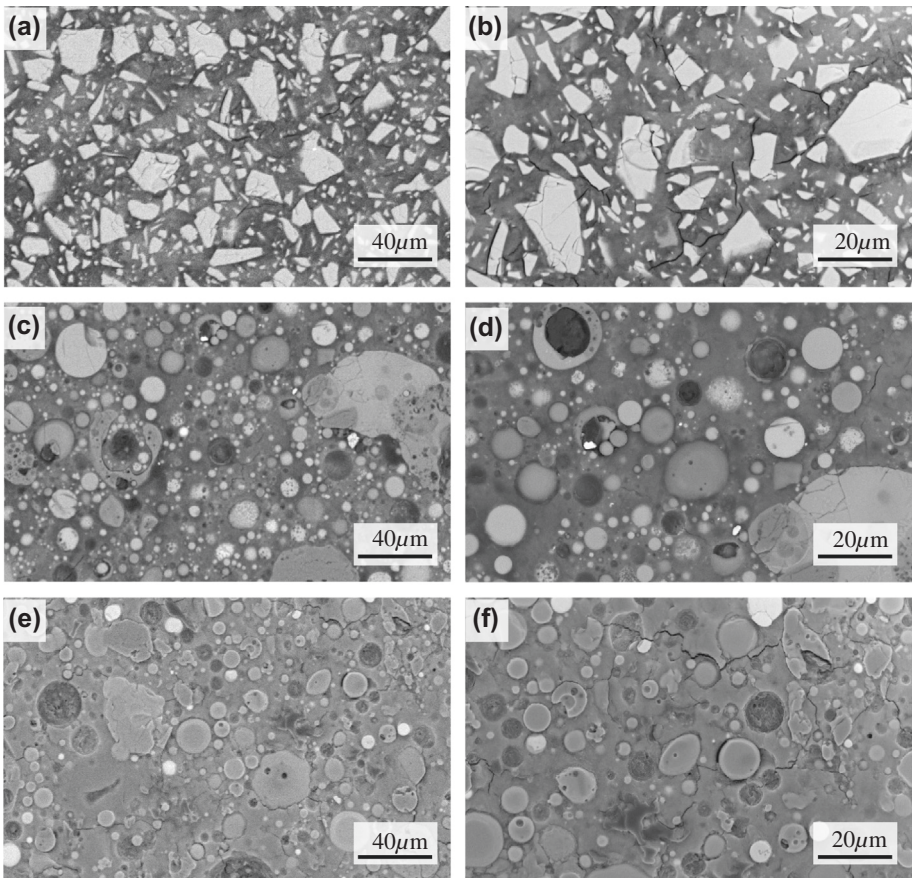

Fig. 6. Backscatter SEM mode images of alkali-activated binder formed from slag (a and b), class C fly ash (c and d), and class F fly ash (e and f) mixed with alkaline solution that contributes 7 wt.% Na_2O (1.5 SM) with respect to starting material at a solution-to-starting material ratio of 0.45, and curing for (a and b) 1 or (c–f) 2 days at 50 °C.

the chemical composition of the class F fly ash is more heterogeneous than that of the slag. Furthermore, there is evidently a greater proportion of porous unreacted or partially reacted particles in the class C fly ash based systems than in the class F fly ash based systems. EDX analysis reveals that these particles are richer in calcium than are the non-porous unreacted and partially reacted particles. This morphological difference between class C and class F fly ash may have significant implications for the development of microstructural properties in the two systems that impact their relative macroscopic performance.

The dissolution of CaO from the outer surfaces of the calcium rich C-FA particles is likely to expose more reactive aluminum oxide that would otherwise have been largely inaccessible to the activating solution. As a result, more aluminum ions would enter the surrounding solution in the C-FA based system than in the F-FA based system, where the lack of calcium in the starting material precludes this mechanism from dominating. Lee and van Deventer [36] found that more Ca, Al, and Si dissolved from the fly ash particles into the highly alkaline (~13.95 pH) leaching solution earlier on in the reaction process at room temperature with increase in soluble silicate concentration and silica modulus (0.356–0.949) in the sodium silicate leaching solution (see Table 2 in their work, specifically the results for F,G, and H). In the systems studied in this current study, with an even higher silica modulus (1.5) and curing temperature (50 °C) [17], it may be expected that the dissolution of the vitreous portions of the starting material occurs at still earlier times and at higher rates. The higher dissolution of Ca and Al into solution in the C-FA system would suggest that more aqueous species become available for binding gel formation than in the case of the F-FA based binding system. The presence of more species for gel formation leads to a denser gel matrix, which has previously been correlated with higher strength development [37].

There does not appear to be much, if any, significant difference in the microstructural morphology of the unreacted particle-binding gel system for a given starting material when the activator concentration is changed from 5% to 7% Na_2O. The Si/Al ratio of the gel for these two cases falls in the range greater than or equal to 1.65, which Duxson et al. found to correlate with a highly homogenous matrix in the case of sodium silicate activated metakaolin based geopolymers (i.e. Al/Si less than or equal to 0.61) [33]. In each of the six mixtures, a large fraction of unreacted particles remains. Despite extensive micro-cracking in the slag based binders, these proved to be twice as strong as the next strongest of the binders (C-FA). The cracking in the 7% Na_2O-activated slag system appears to be less severe compared with that in the 5% Na_2O activated system. This may be related to the higher water-to-solids ratio of the 5% Na_2O slag mixture compared to that of the 7% Na_2O slag mixture. As a result, more pores may be left and emptied during curing at 50 °C. The authors are not confident, however, that this partially or fully explains the 40 MPa difference in compressive strength between the two binders. The cracking observed may also be due to heat treatment of these characterization specimens after exchanging the pore solution with 2-Propanol. The higher water content in the 5% Na_2O slag system may have resulted in more liquid-filled pores left after activation, meaning more water available for solvent exchange and therefore more cracking potential (during subsequent drying of the specimen before epoxy impregnation). However, the causes of cracking and any prevention mechanisms need to be studied further, in detail, for these types of systems.

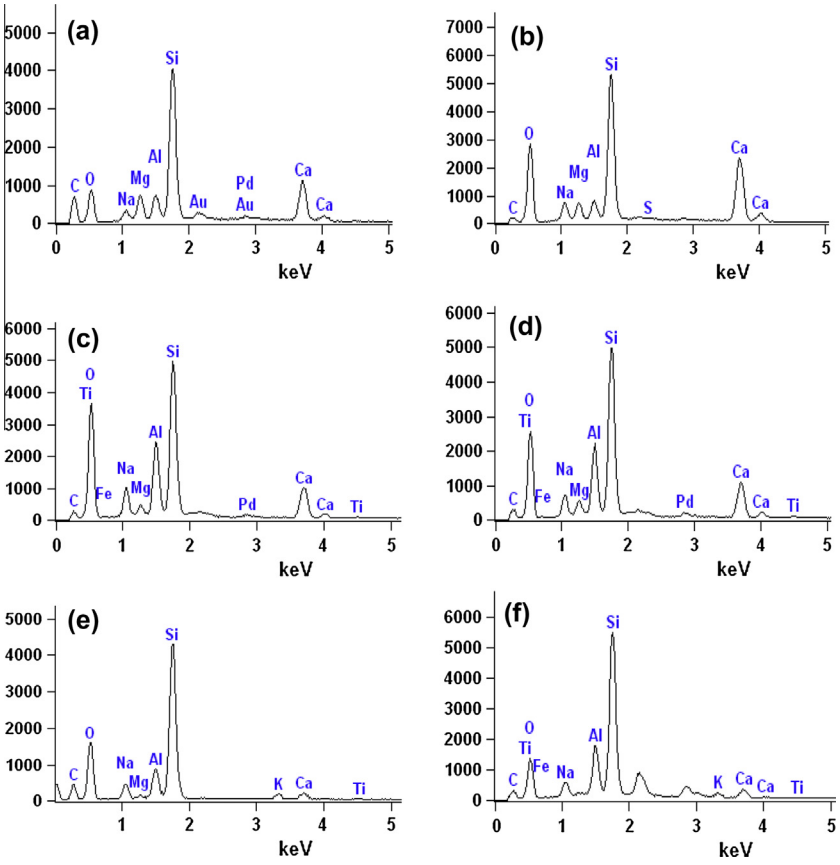

Fig. 7. Representative EDX micrographs of gel matrix composition in the (a) 5% Na_2O activated slag, (b) 7% Na_2O activated slag, (c) 5% Na_2O activated class C fly ash, (d) 7% Na_2O activated class C fly ash, (e) 5% Na_2O activated class F fly ash and (f) 7% Na_2O activated class F fly ash systems.

3.4. Gel composition

A typical EDX spectrum of the gel that forms in each of the six binders studied is shown in Fig. 7. As may be observed from these graphs, the gel products that form in the slag based binders (Fig. 7(a and b)) contain mostly Si, Ca and O, while the C-FA (Fig. 7(c and d)) and F-FA (Fig. 7(e and f)) based binders contain mostly Si and Al, in addition to O. The Ca/Si ratio is highest for slag and lowest for F-FA. The ratio of Al to Si is highest in the C-FA binders, followed by the F-FA binders and then by the slag binders. Minor amounts of Mg and Na were detected in the EDX spectra of all the samples, and traces of Ti, K and Fe were also visible in the EDX spectra of fly ash samples. The amount of Na incorporated in the slag based gel is less than or equal to the amount of Mg in the same gel, while much more Na is present than Mg in each of the fly ash-based gels. EDX points were collected using a NORAN System Six X-ray Microanalysis software package, which then converted the raw data into atomic% composition. The discussion in this section comparing the elemental ratios in the binders studied is based on the atomic% element ratios, which are presented in Fig. 8.

Fig. 8(a–d) shows the atomic% Na/Si, Al/Si and Ca/Si ratios for the gel matrix that formed in each of the six mixtures characterized in this study plotted against one another. When the activator concentration increased from 5% Na_2O (7.5% SiO_2) to 7% Na_2O (10.5% SiO_2), the Ca/Si ratio in F-FA based binder decreased from an average of about 0.2 to an average of about 0.075. This was expected due to the low amount of Ca in the class F fly ash (see Table 1), which is too small to compensate for the increase in soluble silica in the activating solution available for incorporation into the binder. As may be deduced from Fig. 8(c and d), the average Al/Si ratio in F-FA based binder decreases slightly with increase in activator concentration (soluble SiO_2 and Na_2O), though it appears that there is less variation in the 7% Na_2O activated system. The same trend is observed for the Na/Si ratio (see Fig. 8(a and b)), which supports the previous finding that a relatively narrow ratio of Na/Al exists in the network structure of alkali-aluminosilicate gel due to the charge balancing requirement of Al^{3-} that Na^+ fulfills [33].

In contrast to the F-FA based systems, the slag based binders show an increase in Ca/Si ratio with increase in activator concentration. The raw data (net counts) shows that there is decidedly more calcium present in the 7% Na_2O slag system than in the 5% Na_2O slag system. This could be due to a higher initial CaO dissolution rate in the system of higher Si and Na concentrations (higher initial solution pH). Since reactive CaO is the most abundant chemical compound in slag, this may be a reasonable postulation. The Na/Si ratio appears to increase with increasing activator concentration, from an average of about 0.15 to about 0.3. Higher concentrations of Na and Si in the activator enhance the dissociation and reaction of the slag grains, thereby resulting in a higher amount of Ca in the hydrated product. There is no apparent variation in the Al/Si ratio with increase in activator concentration, which suggests that more aluminum ions dissolved from the slag grains in the presence of higher pH and soluble silica (the atomic% inclusion of Si in the binder formed by using the two different activators does not vary significantly; neither do the net counts for Si. The atomic% inclusion of Al also does not vary significantly, however the net counts decrease significantly with increase of activator concentration). This may suggest that a lower quantity of reactive silica from slag grains dissociates into solution with the increase in activator concentration or that more of the dissolved silica prefers to remain in solution rather than to condensate from the solution. It appears that the 7% Na_2O activator has yielded higher

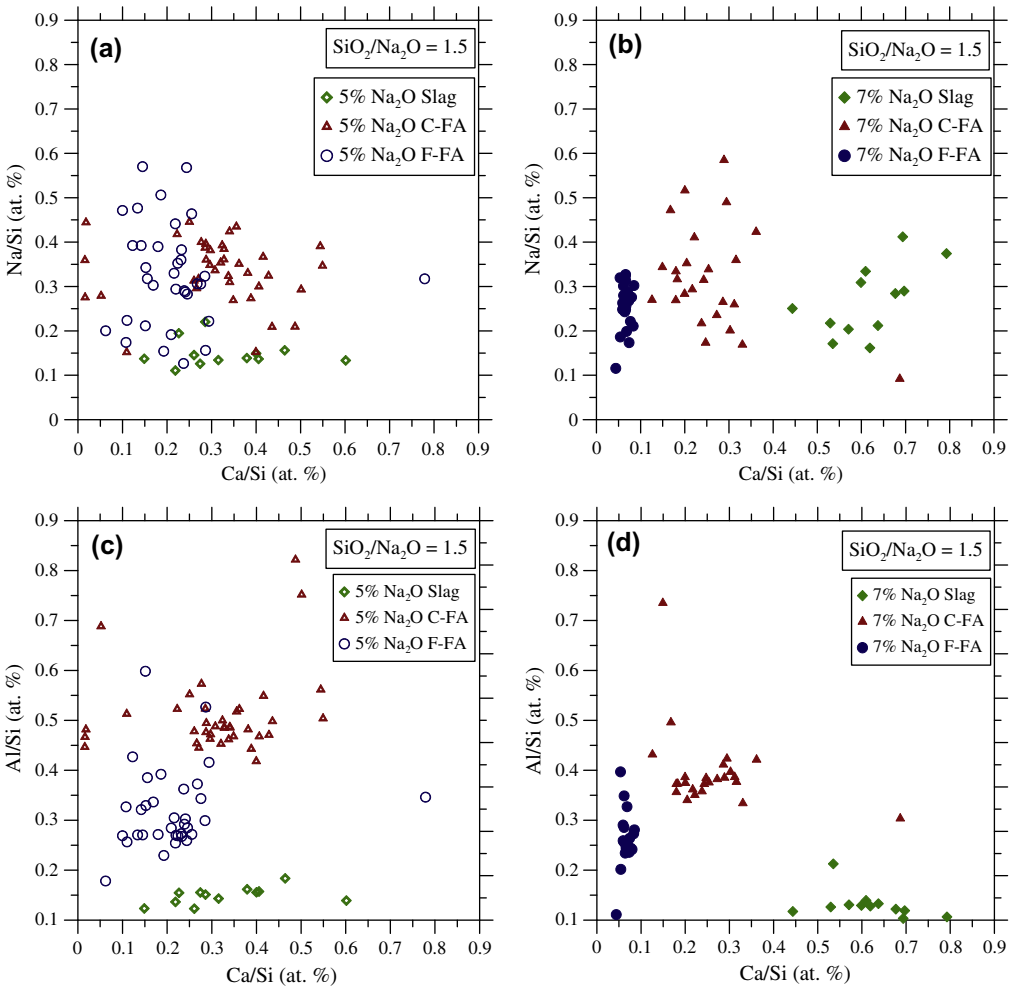

Fig. 8. Atomic ratios of alkali-activated class F fly ash, class C fly ash, and slag (5% and 7% Na_2O, 1.5SM, 0.45 solution-to-starting material ratio, cured for 1 day (slag) and 2 days (fly ash) at 50 °C).

incorporation of the different dissociated ions (besides silicon) from slag and from the activator itself.

The behavior of the C-FA systems seems to be more complicated than that of the slag and F-FA systems. There appears to be a coexistence of two types of gel products in the 5% Na_2O activated binder; one with a low Ca/Si ratio, and the other with a Ca/Si ratio range that overlaps entirely with that of the analogous slag system. The low-calcium gel in this binder has an even lower Ca/Si atomic% ratio than that in the 5% Na_2O F-FA based binder. When the activator concentration is increased from 5% to 7% Na_2O, the Ca/Si ratios converge to a smaller range with an average of about 0.225, which is lower than that of the corresponding slag system (0.5) and higher than that of the corresponding F-FA system (0.075). The Na/Si ratio appears to increase for slag and C-FA based systems and to decrease for F-FA based systems with increase in activator concentration. This would indicate that significantly more Si ions dissociate from class F fly ash particles with increase of activating solution pH, as has been previously mentioned, or that it becomes more thermodynamically favorable for the silicon species in solution to condensate.

The Al/Si ratio in the C-FA based system decreases somewhat from an average of about 0.5 to about 0.375, with increase in activator concentration. This may indicate that any increase in the reactive aluminum's dissolution rate that resulted due to increased solution pH did not compensate for the increase in the activator's soluble silica concentration. This trend may also be due to a significantly higher rate of Al^{+3} ion accumulations near particle surfaces, decreasing the local pH and therefore further Al dissolution. There may also be more rapid formation of products near particle surfaces, decreasing the exposure of unreacted particle surfaces to alkaline solution, thereby inhibiting further ion dissolution.

The aluminum incorporation into the binder gel appears to be greater in C-FA systems than in F-FA systems, despite the fact that there is slightly more aluminum present in the F-FA than in the C-FA. A potential explanation for this, as discussed earlier, is that more aluminum oxide in fly ash particles may be exposed to high pH solution upon dissolution of calcium from the outer surfaces of C-FA particles, and therefore more Al becomes available for gel product formation in C-FA systems compared to F-FA systems.

The Na/Al ratio of gels from C-FA system is approximately equal to one when activated with the 7% Na_2O solution but is less than one when activated with the 5% Na_2O solution. This may suggest that the solvent pH in the 5% Na_2O C-FA system is high enough for a large proportion of the accessible Al in the fly ash to dissolve into the solution and subsequently be incorporated into the gel products. When more Na is added to the system with increase in activator Na_2O concentration, the ratio between Na and Al increases. This would indicate that the increase in Na to the liquid is greater than the increase in Al dissolution into the liquid.

Referring to Table 1, the sum of $K_2O + Na_2O + MgO$ in the starting material is equal to 11.1 wt.%, 6.2 wt.%, and 3.4 wt.% for slag, class C fly ash and class F fly ash, respectively. This trend further exaggerates the trend among the three starting materials with respect to calcium content. X-ray mapping, not displayed in this

paper, shows that Mg is present in significant amounts in the binding gel in class C fly ash based systems, while not as much is found in class F fly ash based geopolymer gel. From this observation, it may be postulated that the additional alkalis and MgO present in the calcium rich starting materials contribute to almost immediate increased pH and therefore increased dissolution rates of the Ca, Si, and Al ions into solution. Also, increased alkalis in solution may contribute to more formation of gel products by substituting for Ca and Na in the assumed N–A–S–H and C–A–S–H gel microstructures.

4. Conclusions

The following conclusions may be drawn from the results of this study regarding the effect of starting material and alkaline activator concentration on the hydration kinetics, strength development and composition of the resulting binding gel. Though characterized by lower heat evolution and shorter induction periods that decrease with increasing activator concentration, the heat flow profiles of alkali-activated slag-based binding systems resemble those of traditional OPC systems. The analogous fly ash-based systems behave very differently, exhibiting only one initial peak and no induction period. Strength development and cumulative heat is greater in systems whose starting materials contain more calcium. Alkali activated F-FA based systems require a higher activator concentration in order to react to form a binder of adequate compressive strength for practical structural use compared to the requirements of systems based on the other two starting materials. Though the alkali-activated C-FA based systems developed adequate compressive strength, their quick setting times remain a practical hindrance that needs to be resolved before their implementation as structural materials can reasonably proceed. A continuous gel matrix formed in each binding system, irrespective of starting material and activator concentration, even in the binder whose compressive strength was below 30 MPa. The pH of and available Na_2O and soluble SiO_2 in the activator seems to have a significant influence on the type(s) of gel phase that forms in alkali activated C-FA based binder systems. When the pH of the activator is slightly below 13, the system favors the coexistence of two gel phases (likely C (N)–A–S–H and N–A–S–H gels). However, when the pH of the activator equals or exceeds 13.3, the system favors the persistence of only one gel phase whose Ca/Si ratio falls between that of analogous F-FA and slag binder gels. Finally, the Ca/Si ratio of the gel in slag based alkali activated binders increases with increasing activator pH.

Acknowledgments

The authors would like to acknowledge the financial support from the National Science Foundation through the CAREER Grant Award No. 1055641. Additionally, Holcim (USA) Inc., Lafarge North America, and Graymont Stone and Concrete are acknowledged for providing slag, class C fly ash and class F fly ash, respectively, for this research.

References

[1] Juenger MCG, Winnefeld F, Provis JL, Ideker JH. Advances in alternative cementitious binders. Cem Concr Res 2011;41(12):1232–43.
[2] Lothenbach B, Scrivener KL, Hooton RD. Supplementary cementitious materials. Cem Concr Res 2011;41:217–29.
[3] Mehta KP, Monteiro PJM. Concrete microstructure, properties, and materials. 3rd ed. New York: McGraw-Hill; 2006.
[4] Wang S, Pu X, Scrivener KL, Pratt PL. Alkali-activated slag cement and concrete: a review of properties and problems. Adv Cem Res 1995;7(27):93–102.
[5] Scrivener KL, Nonat A. Hydration of cementitious materials, present and future. Cem Concr Res 2011;41:651–65.
[6] Duxson P, Fernández-Jiménez A, Provis JL. Geopolymer technology: the current state of the art. J Mater Sci 2007;42(9):2917–33.
[7] Tempest B, Sanusi O, Gergely J, Ogunro V, Weggel D. Compressive strength and embodied energy optimization of fly ash based geopolymer concrete. WOCA Conf. <http://www.flyash.info/>; 2009 [accessed 26.06.13].
[8] Roy DM. Alkali-activated cements opportunities and challenges. Cem Concr Res 1999;29(2):249–54.
[9] Malhotra VM. Making concrete "greener" with fly ash. supplementary cementing materials can reduce greenhouse gas emissions into the environment. Concr. Int. 1999;21(5):61–6.
[10] Mehta K. Concrete technology for sustainable development. Concr. Int. 1999;21(11):47–53.
[11] Duxson P, Provis JL, Lukey GC, van Deventer JSJ. The role of inorganic polymer technology in the development of 'green concrete'. Cem Concr Res 2007;37(12):1590–7.
[12] Duxson P, Provis JL. Designing precursors for geopolymer cements. J Am Ceram Soc 2008;91(12):3864–9.
[13] Habert G, d'Espinose de Lacaillerie JB, Noussel N. An environmental evaluation of geopolymer based concrete production: reviewing current research trends. J Clean Prod 2011;19(11):1229–38.
[14] Hardjito D, Rangan BV. Development and properties of low-calcium fly ash-based geopolymer concrete. Res Rep GC 2005;1.
[15] Fernández-Jiménez A, Palomo A. Composition and microstructure of alkali activated fly ash binder: effect of the activator. Cem Concr Res 2005;35(10):1984–92.
[16] Haha MB, Lothenbach B, Le Saout G, Winnefeld F. Influence of slag chemistry on the hydration of alkali-activated blast-furnace slag — Part II: Effect of Al_2O_3. Cem Concr Res 2012;42(1):74–83.
[17] Guo X, Shi H, Dick WA. Compressive strength and microstructural characteristics of class C fly ash geopolymer. Cem Concr Compos 2010;32(2):142–7.
[18] Palomo A, Grutzeck MW, Blanco MT. Alkali-activated fly ashes: a cement for the future. Cem Concr Res 1999;29(8):1323–9.
[19] Haha BM, Le Saout G, Winnefeld F, Lothenbach B. Influence of activator type on hydration kinetics, hydrate assemblage and microstructural development of alkali activated blast-furnace slags. Cem Concr Res 2011;41(3):301–10.
[20] Provis JL, Lukey GC, van Deventer JSJ. Do geopolymers actually contain nanocrystalline zeolites? A reexamination of existing results. Chem Mater 2005;17(12):3075–85.
[21] Provis JL, van Deventer JSJ, editors. Geopolymers: structure, processing, properties and industrial applications. Boston: Woodhead Publishing Limited and CRC Press; 2009.
[22] Ravikumar D, Peethamparan S, Neithalath N. Structure and strength of NaOH activated concretes containing fly ash or GGBFS as the sole binder. Cem Concr Compos 2010;32(6):399–410.
[23] Criado M, Fernández-Jiménez A, Palomo A. Alkali activation of fly ash: effect of the SiO_2/Na_2O ratio Part I: FTIR study. Micropor Mesopor Mater 2007;106:180–91.
[24] Van Jaarsveld JGS, van Deventer JSJ, Lukey GC. The effect of composition and temperature on the properties of fly ash- and kaolinite-based geopolymers. Chem Eng J 2002;89:63–73.
[25] Bernal SA, Provis JL, Rose V, Mejía de Gutierrez R. Evolution of binder structure in sodium silicate-activated slag–metakaolin blends. Cem Concr Compos 2011;33(1):46–54.
[26] Oh JE, Monteiro PJM, Jun SS, Choi S, Clark SM. The evolution of strength and crystalline phases for alkali-activated ground blast furnace slag and fly ash-based geopolymers. Cem Concr Res 2010;40(2):189–96.
[27] Alonso S, Palomo A. Calorimetric study of alkaline activation of calcium hydroxide–metakaolin solid mixtures. Cem Concr Res 2001;31(1):25–30.
[28] Kumar S, Kumar R. Tailoring geopolymer properties through mechanical activation of fly ash. In: 2nd Int Conf Sustain Constr Mater Technol. Ancona, Italy; 2010.
[29] Komnitsas K, Zaharaki D. Geopolymerisation: a review and prospects for the minerals industry. Miner Eng 2007;20:1261–77.
[30] Song S, Jennings HM. Pore solution chemistry of alkali-activated ground granulated blast-furnace slag. Cem Concr Res 1999;29:159–70.
[31] Rothstein D, Thomas JJ, Christensen BJ, Jennings HM. Solubility behavior of Ca-, S-, Al-, and Si-bearing solid phases in Portland cement pore solutions as a function of hydration time. Cem Concr Res 2002;32:1663–71.
[32] Fernández-Jiménez A, Palomo A, Sobrados I, Sanz J. The role played by the reactive alumina content in the alkaline activation of fly ashes. Micropor Mesopor Mater 2006;91:111–9.
[33] Duxson P, Lukey GC, Separovic F, van Deventer JSJ. Effect of alkali cations on aluminum incorporation in geopolymeric gels. Ind Eng Chem Res 2005;44(4):832–9.
[34] Fernández-Jiménez A, Palomo A. Mid-infrared spectrographic studies if alkali-activated fly ash structure. Micropor Mesopor Mater 2005;86:207–14.
[35] Pietersen HS, Fraay A, Bijen JM. Reactivity of fly ash at high pH. Mater Res Soc Symp Proc 1990.
[36] Lee WKW, van Deventer JSJ. Structural reorganisation of class F fly ash in alkaline silicate solutions. Colloid Surf A 2002;211:48–66.
[37] Criado M, Fernández-Jiménez A, de la Torre AG, Aranda MAG, Palomo A. An XRD study of the effect of the SiO_2/Na_2O ratio on the alkali activation of fly ash. Cem Concr Res 2007;37(5):671–9.